RSC Advances

COMMUNICATION

View Article Online
View Journal | View Issue

Cite this: *RSC Adv.*, 2014, **4**, 24453

Received 2nd April 2014
Accepted 23rd May 2014

DOI: 10.1039/c4ra02895c

www.rsc.org/advances

Vacuum processable donor material based on dithieno[3,2-*b*:2′,3′-*d*]thiophene and pyrene for efficient organic solar cells†

Jongchul Kwon,‡[a] Tae-Min Kim,‡[b] Hong-Se Oh,[a] Jang-Joo Kim*[b] and Jong-In Hong*[a]

We have developed a new donor material, 2,6-di(pyren-1-yl) dithieno [3,2-*b*:2′,3′-*d*]thiophene (**DDT**), consisting of dithieno[3,2-*b*:2′,3′-*d*]-thiophene (DTT) and pyrene units. The bulk heterojunction (BHJ) device based on **DDT** : C_{70} = 1 : 4 exhibited an efficient power conversion efficiency (PCE) of 3.60%, under simulated AM 1.5 solar irradiation at 100 mW cm^{-2}.

Organic solar cells (OSCs) are emerging as a clean and renewable energy resource due to their unique features including low-cost manufacturing, easy synthesis of active layer materials, possibility of flexible panels, easy device fabrication, and other potential applications.[1]

Since the first report of OSCs by Tang,[1] researchers have focused on improving the power conversion efficiency (PCE) of the devices using new organic small molecules. In recent years, the PCE of OSCs has been steadily improved by the use of various organic small molecules.[2–4] Further, the PCEs of 8–9% have been achieved for polymer and small molecule based OSCs with the most promising bulk heterojunction (BHJ) architecture.[5]

Pyrene-based organic materials have been utilized as active materials of organic thin-film transistors (OTFTs), and blue light-emitting and electron-transporting materials in organic light-emitting diodes (OLEDs), and donor materials for OSCs.[6–10] Oligothiophene-based organic materials have been widely investigated for optoelectronic applications such as OSCs, OTFTs, and OLEDs, owing to their light-emitting and absorbing, hole-transporting, and charge carrying transport properties.[11] In particular, linearly fused oligothiophene-based compounds derived from dithieno[3,2-*b*:2′,3′-*d*]thiophene (DTT) have been utilized in a variety of organic optoelectronic applications, because the **DDT** unit has a relatively high hole mobility due to the fused thiophene core.[12–15] Therefore, the synthesis of **DDT** derivatives has received much attention.[16] However, to the best of our knowledge, DTT-based small molecules have not been successfully utilized for high performance OSCs.[17]

In this paper, we report on the development of a thermally stable and efficient donor material, 2,6-di(pyren-1-yl)dithieno [3,2-*b*:2′,3′-*d*]thiophene (**DDT**), consisting of DTT and pyrene units, for OSCs. The device performance was optimized at **DDT** : C_{70} = 1 : 4; the maximum open circuit voltage (V_{oc}), short circuit current (J_{sc}), and PCE value of the device were 0.98 V, 9.24 mA cm^{-2}, and 3.60%, respectively, under simulated AM 1.5 solar irradiation at 100 mW cm^{-2}.

Compound **DDT** was synthesized by the palladium catalyzed Suzuki cross coupling reaction between 2,6-dibromodithieno [3,2-*b*:2′,3′-*d*]thiophene[18] and 1-pyreneboronic acid (Scheme 1). Compound **DDT** was identified by HR-mass and EA analyses.

Fig. 1a shows the absorption (UV) and emission (PL) spectra of **DDT** in CH_2Cl_2 and in solid film. The UV spectrum of **DDT** in CH_2Cl_2 shows a main absorption band with λ_{max} at 387 nm, which originates from the DTT and pyrene unit. The UV spectrum of **DDT** in solid film shows an absorption maximum band at 412 nm, which is 25 nm red-shifted when compared to the absorption in CH_2Cl_2. The PL spectrum of **DDT** shows maximum bands at 499 nm in CH_2Cl_2 and at 569 nm in film, which is 70 nm red-shifted when compared to the absorption in

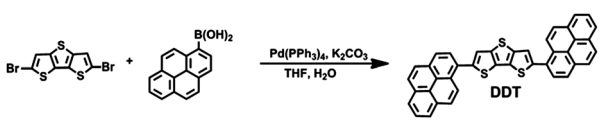

Scheme 1 Synthesis of DDT.

[a]*Department of Chemistry, Seoul National University, Seoul 151-747, Korea. E-mail: jihong@snu.ac.kr; Fax: +82-2-889-1568; Tel: +82-2-874-2456; +82-2-880-6682*

[b]*Department of Materials Science and Engineering and the Center for Organic Light-Emitting Diode, Seoul National University, Seoul 151-742, Korea. E-mail: jjkim@snu.ac.kr*

† Electronic supplementary information available: Detailed experimental procedures, photophysical data, thermal data, electrochemical data, XRD data, device data, and AFM data, additional supporting data. See DOI: 10.1039/c4ra02895c

‡ These authors contributed equally to this work.

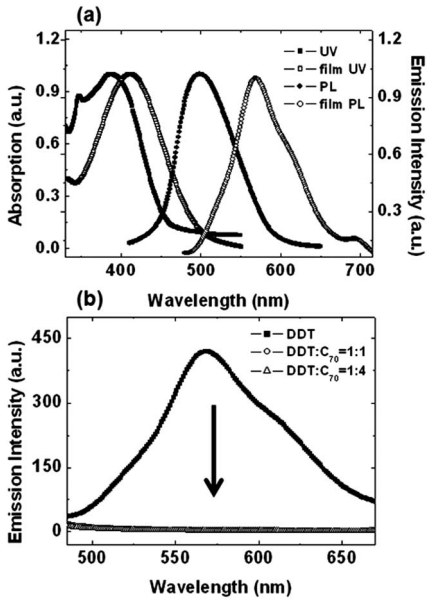

Fig. 1 UV spectra (a) and PL spectra (a and b) of DDT at 400 nm excitation in 0.02 mM CH_2Cl_2 and in solid film.

CH_2Cl_2. The UV and PL spectra of the solid film of **DDT** were both red-shifted relative to the CH_2Cl_2 solution spectra, presumably owing to the more planar structure of **DDT** in the film than in CH_2Cl_2. Fig. 1b and S1† show the PL spectra of **DDT** in neat film and the blended film of **DDT** : C_{70} = 1 : 1, 1 : 4. The PL spectra of **DDT** in **DDT** : C_{70} = 1 : 1, 1 : 4 blended film were significantly quenched by C_{70}. That means that an efficient intermolecular photoinduced charge transfer (PICT) process from the excited state of **DDT** to C_{70} occurred. This PICT process of **DDT** is similar to the case of conducting conjugated polymer and fullerene blend system.[3g]

The thermal stability of **DDT** was investigated by thermogravimetric analysis (TGA) and differential scanning calorimetry (DSC). **DDT** shows a high thermal stability of T_d = 432 °C, as revealed by the TGA thermogram (Fig. 2), suggesting that **DDT** is stable during the vacuum thermal sublimation process used in OSC fabrication. When the sample of **DDT** was heated, a melting peak was observed at around 358 °C (Fig. S2†).

As shown in Fig. S3†, the cyclic voltammograms (CVs) of **DDT** shows irreversible oxidation process in 1,2-dichlorobenzene (ODCB). The oxidation potential energy of **DDT** is observed at E_{onset} = 1.00 V, calibrated against the ferrocene/ferrocenium (Fc/Fc^+) redox couple. The highest occupied molecular orbital (HOMO) energy level of **DDT** (−5.66 eV) is calculated from E_{onset} after correction against the Fc/Fc^+ redox couple. The lowest unoccupied molecular orbital (LUMO) energy level of **DDT** (−2.95 eV) is calculated from the CV and cross sectional wavelength between the UV and PL spectra (Table 1).[19]

DDT-deposited films exhibit no diffraction peaks present in the X-ray diffraction (XRD) patterns, indicating that the **DDT** molecule has poor crystalline morphology in the solid films (Fig. S4, ESI†).

To investigate the correlation between the molecular structure and the photophysical properties, we performed molecular orbital calculations using density functional theory (DFT). The ground state geometries of **DDT** were optimized in vacuum using the B3LYP/6-31 G* level in the Gaussian03 package. The optimized structures and the frontier molecular orbitals are shown in Fig. 3. The HOMO level of **DDT** is located on both the DTT and pyrene units. The LUMO level of **DDT** is mainly located on the pyrene unit.

To investigate the photovoltaic properties of **DDT**, we fabricated planar heterojunction (PHJ) devices with a configuration of ITO/MoO_3 (5 nm)/**DDT** (10, 20, 30 nm)/C_{70} (40 nm)/2,9-dimethyl-4,7-diphenyl-1,10-phenanthroline (BCP) (8 nm)/Al (100 nm). Fig. S5, ESI† shows the current density (*J*) *vs.* voltage (*V*) characteristic curves of the PHJ solar cells. All the PHJ devices exhibit the poor photovoltaic behavior. The optimized 20 nm **DDT**-based device exhibited a J_{sc} of 3.15 mA cm^{-2}, a V_{oc} of 0.76 V, a fill factor (FF) of 0.22; thus a PCE of 0.52% was obtained. In contrast, the device with a 30 nm **DDT** based device had a reduced J_{sc} of 0.71 mA cm^{-2}, a V_{oc} of 0.88 V, and a FF of 0.17; thus, a reduced PCE of 0.11%. The low-lying HOMO energy levels of **DDT** results in a large energy difference relative to the LUMO of fullerenes, leading to the relatively large V_{oc} values. The V_{oc} value increases from 0.60 V to 0.88 V with increasing the thickness of **DDT** film from 10 nm to 30 nm.[20] Overall, the PCE of **DDT**-based PHJ devices were not high compared with other small-molecule-based OSCs due to the short absorption range and poor crystalline property of **DDT** (Fig. S4, ESI†). Fig. S5, ESI† shows the incident photon to current conversion efficiency (IPCE) spectra of PHJ solar cells. PHJ solar cells show IPCE values of 30% at 526 nm for 20 nm **DDT** based device and 25% at 538 nm for 30 nm **DDT** based device (Fig. S5, ESI†).

To improve the PCE, we fabricated bulk heterojunction devices with a configuration of ITO/MoO_3 (5 nm)/**DDT** : C_{70} = 1 : 1, 1 : 4 (50 nm)/BCP (8 nm)/Al (100 nm). Fig. 4a shows

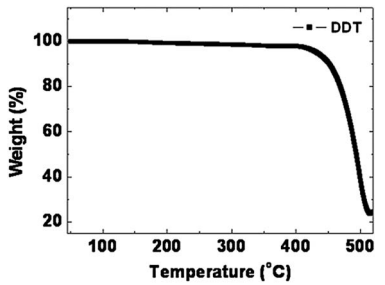

Fig. 2 TGA data of DDT.

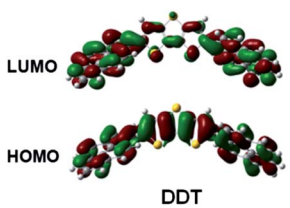

Fig. 3 Electron density distribution of HOMO and LUMO orbital of DDT.

Table 1 Optical, electrochemical and thermal properties of DDT

	UV (nm)		PL (nm)					
	sol	film	sol	film	HOMO (eV)	LUMO (eV)	T_d (°C)	T_m (°C)
DDT	387	412	499	569	5.66	2.95	432	358

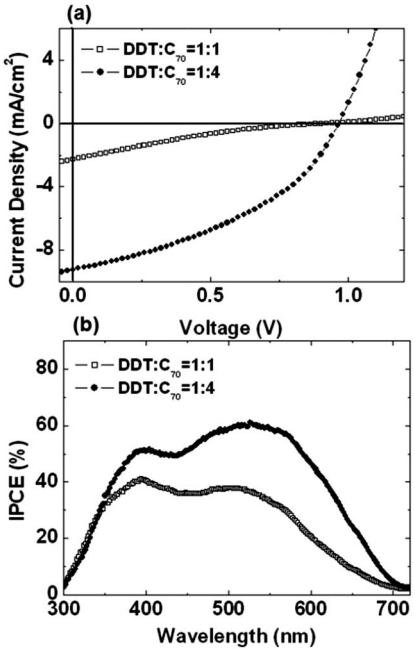

Fig. 4 (a) J–V characteristic curves and (b) IPCE spectra of ITO/MoO_3 (5 nm)/**DDT** : C_{70} = 1 : 1,1 : 4 (50 nm)/BCP(8 nm)/Al (100 nm) device under simulated AM 1.5 solar irradiation at 100 mW cm^{-2}.

the J–V characteristic curves of the BHJ solar cells. The **DDT** : C_{70} = 1 : 1 based device exhibited a J_{sc} of 2.27 mA cm^{-2}, a V_{oc} of 0.91 V, and a PCE of 0.38%. On the other hand, the **DDT** : C_{70} = 1 : 4 based device exhibited a significantly increased efficiency: a J_{sc} of 9.24 mA cm^{-2} a V_{oc} of 0.98 V, and a PCE of 3.60% (Fig. 4a). The higher PCE of the **DDT** : C_{70} = 1 : 4 based device can be explained by the increased dissociation of excitons (Fig. S1, ESI†) and increased carrier mobility at a low donor concentration.[21]

The dependence of the photocurrent (J_{ph}) on the light intensity (I), taken from J–V characteristic curves of the device with **DDT** : C_{70} = 1 : 1 and **DDT** : C_{70} = 1 : 4 (Fig. S6, ESI†), reveals which recombination process is dominant (Fig. 5). The light intensity-dependent photocurrent shows a power law behavior and α is taken from the slope in the log-scale. The devices with **DDT** : C_{70} = 1 : 1 and **DDT** : C_{70} = 1 : 4 show values of α = 0.54 and α = 0.82, respectively. The square-root dependence of the photocurrent on the light intensity in the device with **DDT** : C_{70} = 1 : 1 suggests that the bimolecular recombination process is dominant.[22] In other words, it can be explained that the path for the carrier transport is more or less prevented because of the mixing of the donor and the acceptor molecules. On the contrary, the device with **DDT** : C_{70} = 1 : 4 shows the three-fourth power law dependence of the

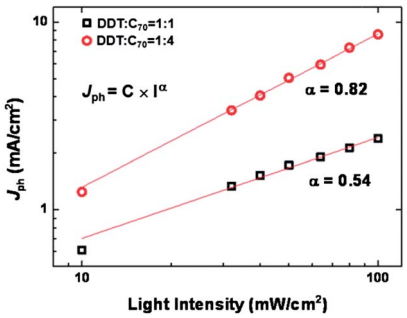

Fig. 5 Incident light intensity dependence of the J_{ph} at the short-circuit condition taken from the J–V characteristic curves of the device with **DDT** : C_{70} = 1 : 1 and **DDT** : C_{70} = 1 : 4 are displayed in black square and red circle, respectively.

photocurrent on the light intensity, which indicates that the space-charge limited recombination process is dominant. This means that the path for the electron and the hole transport is relatively well built in the active layer.[22] It is noteworthy that the PCE of 3.60%, to the best of our knowledge, is the highest value among DTT-based OSC devices due to the efficient exciton dissociation and space charge limited recombination process. Fig. 4b shows the IPCE spectra of BHJ solar cells utilizing **DDT** and C_{70}. The IPCE spectra of the BHJ devices based on **DDT** and C_{70} show a broad response extending from 300 to 700 nm. BHJ devices based on **DDT** : C_{70} show IPCE values with a maximum of 41% at 394 nm for **DDT** : C_{70} = 1 : 1 based device and 60% at 512 nm for **DDT** : C_{70} = 1 : 4 based device (Fig. 4b). The higher PCE and J_{sc} for the device based on **DDT** : C_{70} = 1 : 4 compared to the device based on **DDT** : C_{70} = 1 : 1 is reflected in higher IPCE values in the long wavelength region. The overall device performance data of **DDT** are summarized in Table 2.

In order to explain the device performance difference when using different ratios of **DDT** and C_{70}, we investigated the morphology of these **DDT** : C_{70} blended films by atomic force microscopy (AFM).[23] The AFM images of the blended film of **DDT** : C_{70} are shown in Fig. 6. The morphology of **DDT** film exhibits the formation of an aggregated large domain (Fig. S7, ESI†). The morphology of **DDT** : C_{70} = 1 : 1 blended film exhibits the formation of an aggregated large domain (Fig. 6a). These aggregated domains of **DDT** and **DDT** : C_{70} = 1 : 1 blended films might hinder the efficient exciton dissociation and carrier transport, resulting in low J_{sc} and PCE. On the other hand, the morphology of **DDT** : C_{70} = 1 : 4 blended film exhibits the formation of a relatively small domain (Fig. 6b), which presumably leads to a higher J_{sc} and a high PCE of 3.60%.

Table 2 OSC data based on DDT and C_{70} under simulated AM 1.5 solar irradiation at 100 mW cm^{-2}

Material	V_{oc} (V)	J_{sc} (mA cm^{-2})	FF	PCE (%)
DDT, 10 nm	0.60	1.02	0.16	0.10
DDT, 20 nm	0.76	3.15	0.22	0.52
DDT, 30 nm	0.88	0.71	0.17	0.11
DDT : C_{70} = 1 : 1	0.91	2.27	0.18	0.38
DDT : C_{70} = 1 : 4	0.98	9.24	0.40	3.60

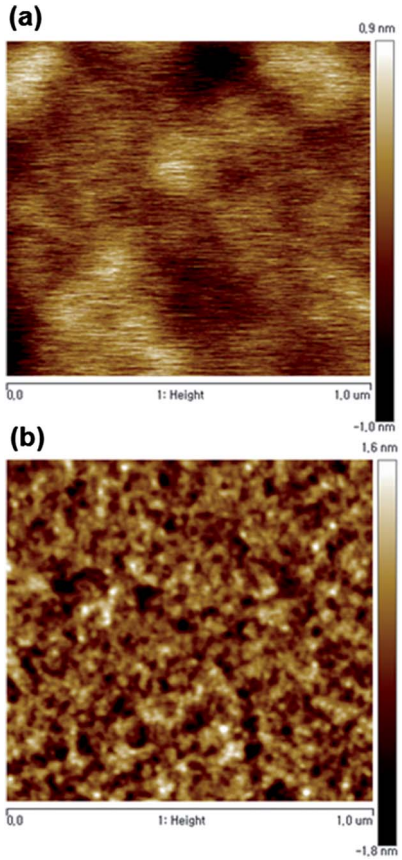

Fig. 6 1×1 μm AFM images of **DDT** : $C_{70} = 1 : 1$ (a) and **DDT** : $C_{70} = 1 : 4$ (b) deposited thin films.

Conclusions

We have demonstrated thermally stable and efficient donor material **DDT**, consisting of **DDT** and pyrene units. The maximum V_{oc}, J_{sc} and PCE values of the BHJ device based on **DDT** : $C_{70} = 1 : 4$ were 0.98 V, 9.24 mA cm^{-2}, and 3.60%, respectively, under simulated AM 1.5 solar irradiation at 100 mW cm^{-2}. A PCE of 3.60%, to the best of our knowledge, is the highest efficiency among OSC devices fabricated using DTT derivatives.

Acknowledgements

This study was supported by a grant from the Basic Science Research Program through the National Research Foundation of Korea (NRF) funded by the Ministry of Education, Science and Technology (MEST) of Korea for the Center for Next Generation Dye-sensitized Solar Cells (no. 2008-0061903), and by the New & Renewable Energy Technology Development Program of the KETEP grant (no. 20113020010070) funded by the Ministry of Knowledge Economy.

References

1 C. W. Tang, *App. Phys. Lett.*, 1986, **48**, 183.
2 A. Mishra and P. Bäuerle, *Angew. Chem., Int. Ed.*, 2012, **51**, 2020.
3 (*a*) B. C. Thompson and J. M. J. Fréchet, *Angew. Chem., Int. Ed.*, 2008, **47**, 58; (*b*) Y. Shirota, *J. Mater. Chem.*, 2000, **10**, 1; (*c*) Y. Shirota, *J. Mater. Chem.*, 2005, **15**, 75; (*d*) J. Roncali, *Acc. Chem. Res.*, 2009, **42**, 1719; (*e*) D. Demeter, T. Rousseau and J. Roncali, *RSC Adv.*, 2013, **3**, 704; (*f*) V. Jeux, D. Demeter, P. Leriche and J. Roncali, *RSC Adv.*, 2013, **3**, 5811; (*g*) N. S. Sariciftci, L. Smilowitz, A. J. Heeger and F. Wudl, *Science*, 1992, **258**, 1474.
4 (*a*) J. Kwon, W. Lee, J.-y. Kim, S. Noh, C. Lee and J.-I. Hong, *New J. Chem.*, 2010, **34**, 744; (*b*) J. Kwon, M. K. Kim, J.-P. Hong, W. Lee, S. Noh, C. Lee, S. Lee and J.-I. Hong, *Org. Electron.*, 2010, **11**, 1288; (*c*) J. Kwon, J.-P. Hong, W. Lee, S. Noh, C. Lee, S. Lee and J.-I. Hong, *Org. Electron.*, 2010, **11**, 1103; (*d*) J. Kwon, M. K. Kim, J.-P. Hong, W. Lee, S. Lee and J.-I. Hong, *Bull. Korean Chem. Soc.*, 2013, **34**, 1355.
5 (*a*) Z. He, C. Zhong, S. Su, M. Xu, H. Wu and Y. Cao, *Nat. Photonics*, 2012, **6**, 593; (*b*) J. Zhou, Y. Zuo, X. Wan, G. Long, Q. Zhang, W. Ni, Y. Liu, Z. Li, G. He, C. Li, B. Kan, M. Li and Y. Chen, *J. Am. Chem. Soc.*, 2013, **135**, 8484.
6 F. Moggia, C. Videlot-Ackermann, J. Ackermann, P. Raynal, H. Brisset and F. Fages, *J. Mater. Chem.*, 2006, **16**, 2380.
7 (*a*) K.-C. Wu, P.-J. Ku, C.-S. Lin, H.-T. Shih, F.-I. Wu, M.-J. Huang, J.-J. Lin, I.-C. Chen and C.-H. Cheng, *Adv. Funct. Mater.*, 2008, **18**, 67; (*b*) J. Kwon, J.-P. Hong, S. Lee and J.-I. Hong, *New J. Chem.*, 2013, **37**, 2881.
8 H.-Y. Oh, C. Lee and S. Lee, *Org. Electron.*, 2009, **10**, 163.
9 T. M. Figueira-Duarte and K. Müllen, *Chem. Rev.*, 2011, **111**, 7260.
10 (*a*) J. Kwon, J.-P. Hong, S. Noh, T.-M. Kim, J.-J. Kim, C. Lee, S. Lee and J.-I. Hong, *New J. Chem.*, 2012, **36**, 1813; (*b*) J.-W. Mun, I. Cho, D. Lee, W. S. Yoon, O. K. Kwon, C. Lee and S. Y. Park, *Org. Electron.*, 2013, **14**, 2341; (*c*) O. P. Lee, A. T. Yiu, P. M. Beaujuge, C. H. Woo, T. W. Holcombe, J. E. Millstone, J. D. Douglas, M. S. Chen and J. M. J. Fréchet, *Adv. Funct. Mater.*, 2011, **23**, 5359.
11 (*a*) J. E. Anthony, *Chem. Rev.*, 2006, **106**, 5028; (*b*) J. E. Anthony, *Angew. Chem., Int. Ed.*, 2008, **47**, 452.
12 X. C. Li, H. Sirringhaus, F. Garnier, A. B. Holmes, S. C. Moratti, N. Feeder, W. Clegg, S. J. Teat and R. H. Friend, *J. Am. Chem. Soc.*, 1998, **120**, 2206.
13 L. Wang, Q. Chen, G. B. Pan, L. J. Wan, S. M. Zhang, X. W. Zhan, B. H. Northrop and P. J. Stang, *J. Am. Chem. Soc.*, 2008, **130**, 13433.
14 L. Zhang, L. Tan, Z. H. Wang, W. P. Hu and D. B. Zhu, *Chem. Mater.*, 2009, **21**, 1993.
15 X. W. Zhan, Z. A. Tan, E. J. Zhou, Y. F. Li, R. Misra, A. Grant, B. Domercq, X. H. Zhang, Z. S. An, X. Zhang, S. Barlow, B. Kippelen and S. R. Marder, *J. Mater. Chem.*, 2009, **19**, 5794.
16 J. Frey, A. D. Bond and A. B. Holmes, *Chem. Commun.*, 2002, 2424.
17 J. K. Lee, S. Lee and S. J. Yun, *Bull. Korean Chem. Soc.*, 2013, **34**, 2148.
18 T.-H. Kwon, V. Armel, A. Nattestad, D. R. MacFarlane, U. Bach, S. J. Lind, K. C. Gordon, W. Tang, D. J. Jones and A. B. Holmes, *J. Org. Chem.*, 2011, **76**, 4088.

19 (*a*) J. Kwon, T.-H. Kwon, H. S. Cho, M. K. Kim, I.-S. Shin, D.-Y. Shin, S. J. Park and J.-I. Hong, *New J. Chem.*, 2008, **32**, 1368; (*b*) M. K. Kim, J. Kwon, T.-H. Kwon and J.-I. Hong, *New J. Chem.*, 2010, **34**, 1317.

20 M. D. Perez, C. Borek, S. R. Forrest and M. E. Thompson, *J. Am. Chem. Soc.*, 2009, **131**, 9281.

21 (*a*) M. Zhang, H. Wang, H. Tian, Y. Geng and C. W. Tang, *Adv. Mater.*, 2011, **23**, 4960; (*b*) Y.-q. Zheng, W. J. Potscavage, Jr, T. Komino, H. Hirade, J. Adachi and C. Adachi, *Appl. Phys. Lett.*, 2013, **102**, 143304.

22 (*a*) I. Riedel, J. Parisi, V. Dyakonov, L. Lutsen, D. Vanderzande and J. C. Hummelen, *Adv. Funct. Mater.*, 2004, **14**, 38; (*b*) L. J. A. Koster, V. D. Mihailetchi, H. Xie and P. W. M. Blom, *Appl. Phys. Lett.*, 2005, **87**, 203502; (*c*) V. D. Mihailetchi, J. Wildeman and P. W. M. Blom, *Phys. Rev. Lett.*, 2005, **94**, 126602.

23 J.-Y. Pan, L.-J. Zuo, X.-L. Hu, W.-F. Fu, M.-R. Chen, L. Fu, X. Gu, H.-Q. Shi, M.-M. Shi, H.-Y. Li and H.-Z. Chen, *ACS Appl. Mater. Interfaces*, 2013, **5**, 972.